

Higher order corrections to bound state energy levels in QED: an effective field theory approach

Patrick Labelle

Department of Physics, McGill University
3600 University St., Montréal, Qc H3A-2T8 Canada

September 14, 2018

Abstract

In [1], a new method was developed to calculate energy levels in QED nonrelativistic bound states, up to order $m\alpha^5$ (or α^3 with respect to the Bohr levels). Whether or not this method could be used beyond this order was left as an open question. In this paper, we answer this question with the help of a nonrelativistic effective field theory, NRQED. This theory permits to deal separately with bound state physics (taking place at momenta of order $m\alpha$ or below) from relativistic physics (where the momentum is of order the electron mass) in a rigorous and systematic manner. We find that, aside from infrared terms which had to be discarded without justification in [1], the $\mathcal{O}(m\alpha^4)$ and $\mathcal{O}(m\alpha^5)$ calculations give the same results in both methods. It is shown, however, that this is due to the special physical origin of these contributions and that the method of [1] would not give the right answer at order $m\alpha^6$ or higher. The separation of scales provided by NRQED is essential to the derivation of this result.

1 Introduction

In [1], fine and hyperfine splittings calculations of nonrelativistic QED bound states are carried out up to order $m\alpha^5$, or α^3 with respect to the lowest order

(Bohr) energy levels. The shifts in energy are obtained, essentially, by sandwiching Feynman scattering amplitudes between Schrödinger wavefunctions. These amplitudes are evaluated with the external particles on mass-shell and their four-momenta taken in the nonrelativistic limit. The authors left open the question of whether this approach could be pushed beyond this order.

In this paper, we answer this question using a nonrelativistic effective field theory, nonrelativistic quantum electrodynamics (NRQED)[2]. The use of such an effective theory is possible because the typical QED bound state momentum is of order $\mu\alpha$ (where μ is the reduced mass), which is much smaller than the masses of the constituents. In an effective field theory, an infinite number of nonrenormalizable interactions are present, but they are suppressed by factors of $1/\Lambda$ where Λ is an appropriate cutoff characterizing a scale of energy at which the theory would break down. Because of the nonrelativistic nature of the bound states we are considering, it is natural to take this cutoff as being the reduced mass of the system. It is important to emphasize that the physics taking place at energies beyond the cutoff Λ *does* affect the low energy physics and thus must not be thrown away. However, because this physics takes place at such a high energy (in comparison to the domain of energy in which the effective theory is used), it can be incorporated back in the low energy theory by renormalizing its coefficients. Let us emphasize that this procedure is performed in a rigorous and systematic way and that the low energy theory can thus be made to reproduce QED to an arbitrary precision (as long as the system under study is characterized by momenta $p < \Lambda$).

We find that the approach of [1] would be inconsistent at the $\mathcal{O}(m\alpha^6)$ and would not lead to the correct shift in energy. Moreover, using NRQED, we will be able to understand why this approach gives the correct order ($m\alpha^4$) and $m\alpha^5$ contributions¹.

This paper is organized as follows. In Section 1, we explain the difficulties associated with QED nonrelativistic bound states. In the following two sections, we show how to build a nonrelativistic effective field theory and why it is particularly useful for the study of bound states. We then evaluate the hyperfine splitting in Positronium up to order $m\alpha^5$ and show what distin-

¹Except for the infrared divergent terms which, in the formalism of [1], must be set aside without any further justification. In the context of NRQED, however, these terms are systematically removed.

guishes the $\mathcal{O}(\alpha^4)$ and $\mathcal{O}(\alpha^5)$ terms from higher order corrections. This will clearly show why the approach of [1] is valid at that order (except for the infrared cutoff dependence), and also why one can generalize the order $m\alpha^5$ result to arbitrary values of n , the principal quantum number. We conclude by explaining how to proceed to obtain the $m\alpha^6$ and higher corrections, and why the approach of Ref.[1] would fail at this stage.

2 Nonrelativistic bound states

In a nonrelativistic bound state, the traditional expansion in the number of loops familiar from quantum electrodynamics (QED) fails. The physical reason is the presence of energy scales absent from scattering theory. Indeed, the finite size of the atom provides an energy scale of order the Bohr radius $\approx 1/m\alpha$ which, by the uncertainty principle, is equal to the inverse of the typical three-momentum of the constituent particle ($\approx m\alpha$). Because of this new energy scale, there is a region of the momentum integration in which the addition of loops will *not* result in additional factors of α . Also, because this energy scale is much smaller than the particles masses, the system is predominantly nonrelativistic, a simplification not taken advantage of in traditional approaches. Moreover, a third energy scale, again vastly different from the previous two, is set by the particles kinetic energies and further complicates bound state calculations. It is at the origin of the so-called retardation corrections which lead, for example, to the Lamb shift.

To illustrate more specifically the problems arising from the presence of these energy scales, consider a traditional Bethe-Salpeter[3] calculation of the energy levels of positronium. The potential in the Bethe-Salpeter equation is given by a sum of two-particle irreducible Feynman amplitudes. One generally solves the problem for some approximate potential and then incorporates corrections using time-independent perturbation theory. Unfortunately, perturbation theory for a bound state is far more complicated than perturbation theory for, say, the electron g -factor. In the latter case a diagram with three photons contributes only to order α^3 . In positronium a kernel involving the exchange of three photons contributes not only to order α^3 , but also to all higher orders as well²:

²We assume here that the Coulomb component of each photon exchange has been projected out. See Section 4 for more details on the special status of the Coulomb interaction

$$\langle V_1 \rangle = \alpha^3 m (a_0 + a_1 \alpha + a_2 \alpha^2 + \dots). \quad (1)$$

Therefore, in the bound state calculation there is no simple correlation between the importance of an amplitude and the number of photons in it. Such behavior is at the root of the complexities in high-precision analyses of positronium or other QED bound states, and it is a direct consequence of the multiple scales in the problem. Any expectation value like Eq.(1) will be some complicated function of the ratios of the three scales in the atom:

$$\langle V_1 \rangle = \alpha^3 m F(\langle p \rangle/m, \langle K \rangle/m). \quad (2)$$

Since $\langle p \rangle/m \sim \alpha$ and $\langle K \rangle/m \sim \alpha^2$, a Taylor expansion of F in powers of these ratios generates an infinite series of contributions just as in Eq.(1). A similar series does not occur in the g -factor calculation because there is but one scale in that problem, the mass of the electron.

Let us again emphasize that traditional methods for analyzing these bound states fail to take advantage of the nonrelativistic character of these systems; and atoms like positronium are very nonrelativistic: the probability for finding relative momenta of $\mathcal{O}(m)$ or larger is roughly $\alpha^5 \simeq 10^{-11}$!

Let us also point out that the difficulties associated with the many different energy scales in bound states are not limited to QED. Consider the study of nonrelativistic QCD bound states, the Υ for example. Even if the means of extracting the properties of such systems, namely simulating the system on a lattice, are very different than the use of the Bethe-Salpeter equation, the nonrelativistic nature of the bound state still greatly complicates calculations. Indeed, the space-time grid used in such a simulation must accommodate wavelengths covering all of the scales in the meson, ranging from $(mv^2)^{-1}$ down to m^{-1} . Given that $v^2 \sim 0.1$ in Υ , one might easily need a lattice as large as 100 sites on side to do a good job. Such a lattice would be three times larger than the largest wavelength, with a grid spacing three times smaller than the smallest wavelength, thereby limiting the errors caused by the grid. This is a fantastically large lattice by contemporary standards and is quite impractical. The strong force equivalent of NRQED, NRQCD[4], greatly reduces the size of the lattices required to study heavy quarks systems since it essentially eliminates the mass of the meson as a relevant energy scale in the calculation (we will soon see how this occurs in NRQED).

in nonrelativistic bound states.

3 NRQED

To take advantage of the simplifications associated with nonrelativistic systems, one can approximate QED in the limit $p/m \ll 1$ (which is equivalent to the limit $v/c \ll 1$). One way to do this consists of simply expanding the QED Lagrangian in powers of p/m to obtain NRQED. The usefulness of this expansion is enhanced by performing a Foldy-Wouthuysen transformation, which decouples the electron and positron degrees of freedom. It is also, however, possible to define NRQED without prior knowledge of QED. Indeed, one can build up the Lagrangian of NRQED by imposing restrictions coming from the symmetry obeyed by the theory, such as gauge invariance, chiral symmetry in the limit $m_e \rightarrow 0$, and Lorentz invariance for the photon kinetic term. Lorentz invariance for the rest of the Lagrangian and renormalizability are *not* necessary.

It is of course possible to write down an infinite number of terms respecting these symmetries, but this is not a problem since operators of dimension greater than 4 will be multiplied by coefficients containing inverse powers of m , the only available energy scale in the problem (remember that m plays the role of the ultraviolet cutoff Λ in NRQED). Since we are considering the limit $p/m \ll 1$, these operators will yield contributions suppressed by that many powers of p/m and therefore, for a given accuracy, only a few terms need to be kept in an actual calculation. The first few terms one obtains are then

$$\begin{aligned}
\mathcal{L}_{\text{NRQED}} = & -1/4(F^{\mu\nu})^2 + \psi^\dagger \left\{ i\partial_t - eA_0 + \mathbf{D}^2/2m + \mathbf{D}^4/8m^3 \right. \\
& + c_1 e/2m \boldsymbol{\sigma} \cdot \mathbf{B} + c_2 e/8m^2 \nabla \cdot \mathbf{E} \\
& \left. + c_3 ie/8m^2 \boldsymbol{\sigma} \cdot (\mathbf{D} \times \mathbf{E} - \mathbf{E} \times \mathbf{D}) + \dots \right\} \psi \\
& + d_1 e^2/m^2 (\psi^\dagger \psi)^2 + d_2 e^2/m^2 (\psi^\dagger \boldsymbol{\sigma} \psi)^2 + \dots \\
& + \text{positron and positron-electron terms.} \tag{3}
\end{aligned}$$

where the c 's and d 's are coefficients of order one. Here, ψ and χ are the (two-component) electron and positron spinors and \mathbf{D} is the gauge-invariant derivative. An example of a positron-electron term (and the one we will focus on later) is $d_3 e^2/m^2 (\psi^\dagger \boldsymbol{\sigma} \chi) \cdot (\chi^\dagger \boldsymbol{\sigma} \psi)$, which represents, to lowest order, the process $e^+e^- \rightarrow e^+e^-$ in the s channel. This term, and the other two having coefficients starting with d 's are examples of “contact” interactions.

Notice that we have recovered the interactions familiar from nonrelativistic quantum mechanics such as the first order relativistic correction to the kinetic energy ($\mathbf{D}^4/8m^3$) and the Darwin term ($c_2 e/8m^2 \nabla \cdot \mathbf{E}$).

Of course, one cannot perform a nonrelativistic expansion of the photon kinetic term. It is however still possible to simplify the nonrelativistic calculation by choosing the most useful gauge in that context, the Coulomb gauge (the reason for its usefulness will become clear later on). In that gauge, the Coulomb propagator is given by i/\mathbf{k}^2 and the transverse propagator is given by

$$\frac{i}{k^2 + i\epsilon} \left(\delta_{ij} - \frac{k_i k_j}{\mathbf{k}^2} \right). \quad (4)$$

The non recoil limit is obtained by setting $k^2 = -\mathbf{k}^2$ in the transverse photon propagator, which amounts to neglecting the energy transferred by the photon.

We now have to fix the coefficients appearing in $\mathcal{L}_{\text{NRQED}}$. To do so, we may simply compare scattering amplitudes in both QED and NRQED, at a given kinematic point (which we choose to be at threshold, *i.e.* with the external particles at rest). This renormalization of the low energy coefficients (often referred to as the “matching procedure” in the literature on effective field theories) must be carried out to as many loops as required for the accuracy desired in the final calculation; at that stage, one can associate a factor of e for each vertex to evaluate the contribution to the bound state calculation (see section [4.1] for more details). Only a finite number of NRQED interactions, for that given number of loops, must be kept. That number is determined using NRQED counting rules, which permit to determine the order at which a given NRQED diagram will contribute, *after* renormalization (or matching) has been carried out. We will give these rules in section [4.1].

4 Bound states diagrams in NRQED

Now that NRQED is completely defined, we can apply it to bound state calculations, where its usefulness is most apparent. To be specific, consider the energy levels of positronium. In a bound state, the expansion in Feynman diagrams of NRQED reduces to conventional Rayleigh-Schrödinger perturbation theory. The “external” wavefunctions of course don’t correspond to free wavepackets but to bound states. In the traditional Bethe-Salpeter for-

malism, the form of these wavefunctions depend on which interactions one desires to include exactly, and which interactions one wants to treat perturbatively. Depending on this choice, the external wavefunctions may be as simple as the Schrödinger wavefunctions or as complicated as the Dirac wavefunctions.

We are now in measure to appreciate the usefulness of the Coulomb gauge. This gauge permits us to keep the simplest interaction for the zeroth order kernel, namely the Coulomb interaction, in which case the Bethe-Salpeter equation reduces to the Schrödinger equation and the wavefunctions are the ones found in any textbook on quantum mechanics. In this calculation we will work only with the $1S$ wavefunction in positronium (reduced mass $\mu = m/2$) which is given, in momentum space, by

$$\Psi(\mathbf{p}) = \frac{8\pi^{1/2}\gamma^{5/2}}{(\mathbf{p}^2 + \gamma^2)^2}, \quad (5)$$

where γ is the typical bound state momentum, equal to $\mu v = m\alpha/2$ in positronium. The ground state energy is $-\gamma^2/2\mu = -m\alpha^2/4$. Physically, an infinite number of Coulomb interactions is incorporated in the wavefunction.

The reason why at least an infinite number of Coulomb kernels must be taken into account in the wavefunction can be easily understood by considering fig.[1a], where a generic bound state diagram is shown. K_1 and K_2 represent some unspecified kernels. We can schematically represent this diagram by

$$\int \frac{d^3k}{(2\pi)^3} F(\mathbf{k}; \mathbf{k}) \quad (6)$$

where $F(\mathbf{p}_1; \mathbf{p}_2)$ is a function including the bound state wavefunctions, the interactions present in the kernels K_1 and K_2 , and the propagator of the electron-positron pair between these two kernels. The arguments \mathbf{p}_1 and \mathbf{p}_2 represent the three-momenta flowing out of the first kernel and into the second one. In figure [1a], $\mathbf{p}_1 = \mathbf{p}_2 = \mathbf{k}$. As explained above, working with the effective field theory means that the electron mass no longer appears as a dynamical energy scale in the NRQED diagrams; this means that m can only appear as an overall factor of the form $1/m^n$ in figure [1a]³. The function F is therefore *independent* of the electron mass; the only energy scale it depends

³In the language of effective field theories (EFT's), NRQED is a decoupling EFT with cutoff scale $\Lambda = m$. The heavy particle being decoupled is the electron's antiparticle so

on is the typical bound state momentum γ , and the ultraviolet cutoff (when it is divergent)⁴.

Let us now consider adding a Coulomb interaction between the two kernels, as in fig.[1b]. In conventional scattering theory, one would conclude that this diagram is of higher order than diagram [1a] because of the factor α coming from the vertices. However, this argument does not hold in a bound state, because the typical momentum flowing through the Coulomb interaction is of order γ . Indeed, consider how the integral Eq.[6] is modified when one adds the Coulomb interaction. It must now be written

$$\begin{aligned} & \int \frac{d^3k d^3l}{(2\pi)^6} \frac{ie^2}{|\mathbf{k} - \mathbf{l}|^2} \frac{i}{(-\gamma^2 - \mathbf{k}^2)/m} F(\mathbf{k}; \mathbf{l}) \\ &= 4\pi m\alpha \int \frac{d^3k d^3l}{(2\pi)^6} \frac{1}{(\gamma^2 + \mathbf{k}^2)(|\mathbf{k} - \mathbf{l}|^2)} F(\mathbf{k}; \mathbf{l}) \end{aligned} \quad (7)$$

where $i/|\mathbf{k} - \mathbf{l}|^2$ is the Coulomb propagator and $im/(-\gamma^2 - \mathbf{k}^2)$ is the non-relativistic propagator for the e^-e^+ pair.

We see that the mass factors out (more about this later!), leaving γ as the only energy scale in the integral. By dimensional analysis, the final result will be of order $\simeq m\alpha$ (the overall factor) divided by $/\gamma$ (from the integral) $\simeq 1$. This shows that in a bound state, adding a Coulomb interaction does not, in fact, lead to a diagram of higher order. This is why one must sum up all Coulomb interactions in the wavefunctions right from the start. This implies the relation expressed in fig.[2] which is nothing else than a diagrammatic representation of the Schrödinger equation.

4.1 Counting rules

The argument we used to show that adding a Coulomb interaction does not increase the order of a bound state diagram is an example of a NRQED

that Lorentz invariance is broken (as expected in a nonrelativistic theory). Of course, there is a positron in NRQED, but it is here an independent particle; it never appears as the negative energy pole of the electron propagator (in the language of time-ordered perturbation theory, there are no Z graphs). Consequently, one can apply the decoupling theorem [5] to NRQED, with the consequence that the heavy scale m will only appear as an overall factor $1/m^n$ in the interactions. One also expects m to enter in the running of the low energy coefficients through logarithms, but this dependence on m will only come from the QED scattering diagrams, through the matching (see section [5.3]).

⁴We will deal with the infrared divergences separately.

counting rule. These rules are extremely important since they permit one to estimate the order of contribution of a diagram without calculating it. Let us first consider non-recoil diagrams⁵. In that approximation, the counting rules are based on the observation that the mass m of the electron always factors out of the integrals so that it no longer represents a relevant energy scale. This is clear since m factors out of the nonrelativistic fermion propagators, as we saw in Eq.[7], and it enters the rules of the NRQED vertices only as an overall factor. We therefore see that the use of NRQED eliminates the relativistic energy scale of the system, which, in the light of the discussion in the introduction, greatly simplifies the analysis.

Starting from this observation, we can recast the discussion of the Coulomb interaction in the following manner: adding a Coulomb interaction between two kernels as in fig.[1] leads to an additional factor of α coming from the vertices and a factor of m coming from the additional fermion propagator. The corresponding overall factor of $m\alpha$ must be canceled by a factor having the dimensions of energy in order to keep the dimensions straight, but since the only energy scale left in the problem is γ , we finally obtain a correction of order $m\alpha/\gamma \simeq 1$. It now becomes obvious that the Coulomb interaction is the only kernel having the property of not increasing the order of a bound state diagram since all the other interactions contain additional factors of $1/m$. Each of these $1/m$ factors will have to be canceled by a corresponding factor of γ , leading therefore to a result of higher order in α .

With these rules, it becomes extremely simple to evaluate the order of the contribution of a given bound state diagram. All we need to know is that the external wavefunctions contribute a factor $m^3\alpha^3$. To obtain the contribution of a given kernel, one has simply to count the number of explicit factors of α (coming from the vertices) and inverse factors of m (coming from the vertices and the e^-e^+ propagators) this diagram contains. After canceling the $1/m$'s with factors of γ , the number of α 's left over give the order of the contribution of the diagram. Consider, for example, inserting a transverse photon (in the non-recoil limit) between two wavefunctions as in fig.[3]. The transverse

⁵In the case of a bound state having equal mass constituents, as positronium, there is no distinction possible between “recoil effects” and the so-called “retardation effects”. This is not, for example, the case in muonium or hydrogen where (sometimes confusing) distinctions are made between non-recoil and non-retardation approximations. What we mean here by the non-recoil approximation is the limit in which the transverse photon does not carry any energy.

photon vertex has one power of e and one power of $1/m$. Taking the two vertices into account, we can conclude that this diagram will contribute to order $m^3\alpha^3 \times \alpha/m^2 \simeq m\alpha^4$ (it is not necessary to multiply by any factor of γ here). The same is true of the annihilation diagram and of the spin-spin interaction as they also contain a factor of $1/m^2$ relative to the Coulomb interaction. Another important observation is that these diagrams will contribute to only one order⁶ in α , in contradistinction with Feynman diagrams in conventional Bethe-Salpeter analysis. It is important to understand that these rules give the order of contribution of a diagram *after* the renormalization of the effective theory has been performed. Indeed, many NRQED bound state diagrams are actually badly divergent in the ultraviolet. The rules give us the order of the finite contributions left over after the NRQED bare coefficients have been renormalized (or, in other words, after matching with QED has been performed).

The situation is only slightly more complicated when one takes into account recoil effects. We will not dwell on this issue here, but let us just mention that they make the kinetic energies K enter as a mass scale and that they are at the origin of the appearance of log's of α which are characteristic of bound states⁷.

Now that we have a way to estimate the order (in powers of α) of the NRQED diagrams contributions, we can go back to the matching of the effective Lagrangian (Eq.[3]) coefficients with QED. As mentioned earlier, this matching is done by evaluating scattering amplitudes evaluated in both theories. There are two expansions involved in this matching: an expansion in number of loops in both QED and NRQED, and an expansion in p/m in NRQED. The number of loops n required is found by simply setting $m\alpha^{3+n}$ equal to the precision desired in the final result (a factor of $m^3\alpha^3$ comes from the wavefunctions and a factor of $1/m^2$ comes from the nonrelativistic normalization of the Feynman amplitudes). For a given number of loops, there is an infinite number of nonrelativistic interactions in the effective theory

⁶We are still limiting ourselves to the non-recoil limit.

⁷To be more precise, the logarithms involve the bound state typical energy scale $\gamma \simeq m\alpha$ and the heavy scale $\Lambda = m$, leading to a result of the form $\ln(m\alpha/m) = \ln \alpha$. This log of m is the one we mentioned earlier when talking about the running of the low energy coefficients. Notice that the infrared cutoff λ always gets canceled while performing the matching because, by construction, the infrared behavior of the effective theory is the same as the one of the full theory.

but, using the counting rules described above, only a finite number must be kept for a given accuracy in the final result. Even if the rules were derived for bound state diagrams, they can be directly applied to the NRQED scattering diagrams *i.e.*, one imagines sandwiching them between wavefunctions and one performs the same power counting. Once again there are strong ultraviolet divergences but let us repeat that the counting rules give us the order at which the diagrams will contribute once the matching of the NRQED coefficients will have been performed (in other words, once the counterterms will have been included).

There is only one exception to the counting rules, and it occurs when a NRQED scattering diagram contains a power-law infrared divergence. In that case, the counting rules must be modified to take into account the presence of a new scale, the infrared cutoff. Take, for example, a scattering diagram which has an overall factor of $m^2\alpha^5$ times an integral $\int d^3k f(\mathbf{k}, \gamma)$. The counting rules would suggest that this diagram will contribute by a term of order $m^2\alpha^5/\gamma = m\alpha^4$ to the bound state calculation but, if it is linearly infrared divergent, it can actually contribute to order $m^2\alpha^5/\lambda = m\alpha^5 (m/\lambda)$. Let us mention that this type of diagrams always contain Coulomb interactions on external legs and the corresponding integrals are trivial to evaluate. All dependence on the infrared cutoff are due to the sensitivity of theory to low momenta. Since, in that region, the effective theory is “engineered” to reproduce the full theory (here, QED), these singularities are always present in the scattering diagrams of both theories so that the renormalized effective couplings are always λ independent.

The use of these rules is better explained with the help of a concrete example. This is what we do in the next section, where we perform an explicit calculation.

5 Positronium hyperfine splitting

5.1 Order $m\alpha^4$

In this section, we will apply NRQED to a specific calculation, namely the hyperfine splitting⁸ (E (triplet state) - E (singlet state)) of ground state positronium. To lowest order, one has the energy levels of the Bohr theory

⁸Which we will denote by “hfs” in the following.

and there is therefore no hfs. To obtain the first non-zero contribution to the splitting, one has to apply first order perturbation theory to the interactions present in the Lagrangian, Eq.[3]. The only interactions that will contribute to the order of interest and that are spin-dependent are

$$c_1 \frac{e}{2m} \boldsymbol{\sigma} \cdot \mathbf{B}, \quad (8)$$

which couples to the transverse photon, and the spin-dependent contact interaction involving the electron and positron degrees of freedom (or “annihilation” diagram)

$$d_3 \frac{e^2}{m^2} \chi^\dagger \boldsymbol{\sigma} \psi \cdot \psi^\dagger \boldsymbol{\sigma} \chi. \quad (9)$$

All the other interactions, because of the presence of additional powers of $1/m$, will not contribute to this order.

Now we must fix the coefficients c_1 and d_3 before computing the hfs. The first coefficient, c_1 , can be determined by evaluating the spin-flipping scattering of an electron from an external field, in the extreme nonrelativistic limit. Or one can also simply look up the Pauli Hamiltonian, which the first few terms of Eq.[3], at tree level, must reproduce. The end result is that $c_1 = 1$. The corresponding Feynman rule, in momentum space, is

$$\pm e \frac{(\mathbf{p}' - \mathbf{p}) \times \boldsymbol{\sigma}}{2m} \quad (10)$$

where \pm correspond to the electron and the positron, respectively, and \mathbf{p}' , \mathbf{p} are the fermion three-momenta after and before the interaction, respectively. The corresponding contribution to the hfs is

$$\begin{aligned} & -i \int \frac{d^3 p d^3 q}{(2\pi)^6} \frac{(8\pi^{1/2} \gamma^{5/2})^2}{(\mathbf{p}^2 + \gamma^2)^2 (\mathbf{q}^2 + \gamma^2)^2} \\ & \psi^\dagger \left[\frac{e}{2m} (\mathbf{q} - \mathbf{p}) \times \boldsymbol{\sigma} \right]_i \psi \chi^\dagger \left[-\frac{e}{2m} (-\mathbf{q} + \mathbf{p}) \times \boldsymbol{\sigma} \right]_j \chi \\ & \frac{-i}{(\mathbf{p} - \mathbf{q})^2} \left(\delta_{ij} - \frac{(\mathbf{p} - \mathbf{q})_i (\mathbf{p} - \mathbf{q})_j}{(\mathbf{p} - \mathbf{q})^2} \right) \end{aligned} \quad (11)$$

where we have approximated the transverse photon propagator $i/(p - q)^2 \simeq -i/(\mathbf{p} - \mathbf{q})^2$. Physically, this corresponds to neglecting the recoil since only momentum, and no energy, is transferred. The corrections to this approximation are of higher order in α .

The second term in the square bracket is zero because of the triple product. We can therefore contract the indices i and j . We then have to spin average the following expression in the ortho and para states:

$$\psi^\dagger[(\mathbf{p} - \mathbf{q}) \times \sigma]\psi \cdot \chi^\dagger[(\mathbf{p} - \mathbf{q}) \times \sigma]\chi.$$

The results are respectively $-2/3(\mathbf{p} - \mathbf{q})^2$ and $2(\mathbf{p} - \mathbf{q})^2$. Taking the first value minus the second to get the hfs, we obtain for the integral

$$\frac{8\alpha\pi}{3m^2} \int \frac{d^3p d^3q}{(2\pi)^6} \frac{(8\pi^{1/2}\gamma^{5/2})^2}{(\mathbf{p}^2 + \gamma^2)^2(\mathbf{q}^2 + \gamma^2)^2} \frac{(\mathbf{p} - \mathbf{q})^2}{(\mathbf{p} - \mathbf{q})^2} = \frac{m\alpha^4}{3}. \quad (12)$$

Since the \mathbf{p} and \mathbf{q} integrals decouple, the calculation is trivial, leading to the famous Fermi splitting[6].

Let us now consider the annihilation interaction. To fix d_3 , we once more turn to the corresponding QED amplitude, namely the tree level annihilation diagram. In the limit of vanishing external three-momenta, and with nonrelativistic normalization for the spinors ($\bar{u}\gamma_0 u = 1$ instead of $2E$), one easily finds that $d_3 = -ie^2/4$. This interaction therefore contributes to the hfs

$$\begin{aligned} i\psi \gg \psi &= i \int \frac{d^3p d^3q}{(2\pi)^6} \frac{(8\pi^{1/2}\gamma^{5/2})^2}{(\mathbf{p}^2 + \gamma^2)^2(\mathbf{q}^2 + \gamma^2)^2} \times \times \frac{-ie^2}{4m^2} \chi^\dagger \sigma \psi \cdot \psi^\dagger \sigma \chi \\ &= i \frac{\gamma^3}{\pi} \times \frac{-ie^2}{4m^2} \chi^\dagger \sigma \psi \cdot \psi^\dagger \sigma \chi \end{aligned} \quad (13)$$

where $\psi \gg \psi$ is to be taken as representing the contact interaction sandwiched between two wavefunctions (see the first diagram of fig.[4]). The spin average of the spinor expression in Eq.[13] gives 2 in the ortho state and zero in the para state (as it must since, by charge conjugation invariance, para-positronium cannot decay to an odd number of photons). The contribution from the one annihilation kernel is therefore the well known result:

$$+ \frac{m\alpha^4}{4}. \quad (14)$$

5.2 Order $m\alpha^5$

So far, everything has been particularly simple. The evaluation of the α^5 corrections, however, is a little bit more involved. First, let us notice that,

according to the counting rules given above, it is not possible to identify any diagram, either in first or second order perturbation theory, that would lead to a contribution of order $m\alpha^5$. As an example, consider the annihilation interaction in second order perturbation theory (*i.e* two of these interactions sewn together). The wavefunctions would decouple from the inner loop and lead to a factor of $|\Psi(0)|^2 = (m\alpha)^3/8\pi$. There would be a factor of $(e^2/m^2)^2$ coming from the two contact interactions, and a factor of m from the nonrelativistic propagator. In all we obtain an overall factor of α^5 times an integral in which the only energy scale left is $\mu\alpha$. The final result will therefore be of order $m\alpha^6$. One can convince oneself that no other diagram can lead to a contribution of order $m\alpha^5$.

Another problem that arises is that, as is well-known from nonrelativistic quantum mechanics, divergences arise when we apply second order perturbation theory to the Lagrangian, Eq.[3].

These two difficulties are closely related since they have their origins in the fact that we have so far entirely neglected relativistic momenta in our analysis. This cannot be correct when one goes beyond first order perturbation theory since loop momenta are allowed to become arbitrarily high. As explained above, the correct way to handle this is to renormalize the “bare” coefficients of NRQED by matching scattering amplitudes in the effective theory with QED diagrams.

We will now illustrate this procedure in more details with the contribution from the annihilation channel, which is represented by Eq.[13] in NRQED. Renormalizing the coefficient of the contact interaction to one loop means that we impose the sum of all one-loop NRQED diagrams involving this interaction to be equal to the corresponding one-loop QED diagrams, as shown in fig.[4]. As explained above, the counting rules tell us that there are no NRQED bound state diagrams contributing to order $m\alpha^6$. We know that the same must hold true for the NRQED scattering diagrams except if there are infrared divergent amplitudes. It turns out that there is indeed such an amplitude here, given by the annihilation interaction followed by a Coulomb exchange. The corresponding integral is equal to

$$\int d^3k \frac{1}{\mathbf{k}^2} \frac{1}{\mathbf{k}^2 + \lambda^2}$$

which can easily be seen to be linearly infrared divergent. It will therefore contribute to order $m^2\alpha^5/\lambda$ and must be included in our calculation.

The correction to the lowest order coefficient of the contact interaction is then equal to the one-loop QED scattering amplitudes minus the NRQED diagram representing the annihilation interaction followed by one Coulomb exchange. It is easy to evaluate the QED diagrams because the external particles are on-shell and at threshold. The result is

$$\frac{ie^4}{2\pi^2 m^2} - \frac{ie^4 m}{4\pi \lambda} \quad (15)$$

for the vertex interaction, after wavefunction renormalization. Notice the linear infrared divergence. It does not appear in the result of the one-loop renormalized vertex function $\Gamma^\mu(p, q)$ in [1] (see Eq.[A20]). This is, however, due to an error in their calculation as can be seen from the fact that their integral Eq.[A17] does contain a linear infrared divergence, divergence that cannot be canceled by the vertex renormalization constant which is only logarithmically divergent in the infrared.

For the diagram containing the one-loop vacuum polarization, we find

$$\frac{ie^4}{9\pi^2 m^2}. \quad (16)$$

The NRQED diagram containing one Coulomb exchange is also easily evaluated and turns out to be

$$- \frac{ie^4 m}{4\pi \lambda} \quad (17)$$

so that $C^{(1)}$ is

$$\left[\frac{i\alpha^2}{4m^2} \left(32 + \frac{64}{9} \right) \right] / \gg \quad (18)$$

where \gg stands for the (spin averaged) lowest order contact interaction, namely $-ie^2/2m^2$.

The contribution to the hfs is then, up to one loop, equal to

$$\begin{aligned} \psi \gg \psi(1 + C^{(1)}) &= \frac{m\alpha^4}{4}(1 + C^{(1)}) \\ &= \frac{m\alpha^4}{4} - \frac{m\alpha^5}{\pi} \left(1 + \frac{2}{9} \right) \end{aligned} \quad (19)$$

which is indeed the correct result[6].

5.3 Order $m\alpha^6$

We now briefly outline the calculation of the order $m\alpha^6$ correction due to the one-photon annihilation diagram. The first thing to do is to renormalize the coefficient of the NRQED contact interaction to two loops, as we did at the one-loop level in fig.[4]. Keeping only the terms of order α^2 , we obtain the following relation

$$\begin{aligned} \gg C^{(2)} &= C^{(1)} \times \text{one loop NRQED diagrams} \\ &+ \text{two loops NRQED diagrams} \\ &\equiv \text{QED two loops diagrams} \end{aligned} \quad (20)$$

where all diagrams are scattering amplitudes evaluated at threshold and, as mentioned above, we are only considering corrections to the one-photon annihilation diagram. One uses once more the counting rules to determine which NRQED diagrams will contribute to $\mathcal{O}(m\alpha^6)$ in Eq.[20], taking into account the fact that $C^{(1)}$ is of order α .

The rhs (the QED calculation) in Eq.[20] will be of the form

$$A + B \ln(\lambda/m) + C \frac{m}{\lambda} + D \frac{m^2}{\lambda^2} \quad (21)$$

where A, B, C and D are constants of order α^2 . On the other hand, the NRQED diagrams will lead to a result of the form

$$A'(\Lambda) + B \ln(\lambda/\gamma) + C \frac{m}{\lambda} + D \frac{m^2}{\lambda^2} \quad (22)$$

where $A'(\Lambda)$ contains a finite piece of order $m\alpha^6$ and ultraviolet divergent terms. All λ -dependent terms are reproduced by the NRQED diagrams so that $C^{(2)}$ is, in the end, infrared finite (but ultraviolet divergent). The final expression for $C^{(2)}$ is therefore

$$\begin{aligned} C^{(2)} &= (A - A'(\Lambda) + B \ln(\alpha/2)) / \gg \\ &= -\frac{2m^2}{ie^2} (A - A'(\Lambda) + B \ln(\alpha/2)). \end{aligned} \quad (23)$$

Notice that, since the NRQED diagrams contain finite pieces, $C^{(2)}$ is *not* simply equal to the infrared finite part of Eq.[21], A .

Once $C^{(2)}$ is computed, the correction to the hfs is found by calculating

$$\begin{aligned}
\psi >< \psi & (1 + C^{(1)} + C^{(2)}) \\
& + \text{one and two loops NRQED bound state diagrams} \\
& = \frac{m\alpha^4}{4} - \frac{m\alpha^5}{\pi} \left(1 + \frac{2}{9}\right) \\
& \quad + B \ln(\alpha/2) + \mathcal{O}(m\alpha^6)
\end{aligned} \tag{24}$$

which is now completely ultraviolet finite. It is easy to understand, heuristically, why all ultraviolet divergences drop out of Eq.[24]. In a nutshell, ultraviolet divergent terms arise in NRQED for momenta of order m or greater. Since these momenta are much bigger than the typical bound state scale $\gamma \simeq m\alpha$, the UV divergences in the NRQED bound state diagrams can be expected to be the same as the ones encountered in the corresponding scattering diagrams. Since, in Eq.[24], each bound state UV divergence is subtracted from the corresponding NRQED scattering divergence, all Λ dependence gets canceled⁹.

To be more explicit, let us consider in more details one specific NRQED diagram. Take, for example, the bound state diagram containing the contact interaction iterated twice (*i.e.* in second order of perturbation theory), as depicted in fig.[5]. It is easy to check that the counting rules predict a contribution of order $m\alpha^6$ for this diagram. However, the explicit expression for this diagram is not well-defined as it diverges linearly:

$$\begin{aligned}
& \int \frac{d^3p d^3q d^3k}{(2\pi)^9} \frac{64\pi\gamma^5}{((\mathbf{k} - \mathbf{p})^2 + \gamma^2)^2 (\mathbf{q}^2 + \gamma^2)^2} \left(\frac{e^2}{4m^2}\right)^2 \\
& \quad \frac{1}{-\gamma^2/m - \mathbf{p}^2/m} \left(\chi^\dagger \sigma_i \psi \text{Tr}(\sigma_i \sigma_j) \psi^\dagger \sigma_j \chi \right) \Big|_{spin0}^{spin1} \\
& = -\frac{m\alpha^5}{4\pi} \Lambda/m + \frac{m\alpha^6}{8}
\end{aligned} \tag{25}$$

where we have put a cut-off Λ on the three-momentum flowing through one of the contact interaction. This divergence arises from the fact that the

⁹Strictly speaking, this is true only for the power-law UV divergences. The heavy scale is (implicitly) present in Eq.[24], where it cancels the m of the γ factor in the logarithm. See our previous footnote on the running of the low energy coefficients. For a discussion of the issue of power-law divergences in a broader context, see [7].

Lagrangian Eq.[3] is defined for momenta much smaller than the electron mass whereas the momentum in a loop is allowed to become relativistic. However, for $p \geq m$, one expects the intermediate state loop to shrink to a point (in coordinate space), as far as the low energy theory is concerned. This means that the divergent contributions to the NRQED bound state diagrams can be canceled by a renormalization of the tree level coefficients. In fact, the necessary counterterms are already present in the coefficients $C^{(1)}$ and $C^{(2)}$. To see this, let us go back to the definition of $C^{(1)}$, fig.[4]. When we calculated the $m\alpha^5$ correction, the only one-loop NRQED diagram we kept in this equation was the contact interaction followed by a Coulomb exchange. Now, however, in order to be consistent in our calculation of order $m\alpha^6$, we must go back to that equation and include all necessary NRQED one-loop diagrams. One of those diagrams turns out to be the scattering diagram containing the contact interaction iterated twice (*i.e* fig.[5] with free spinors on the external legs instead of wavefunctions), which has the simple Feynman rule

$$- \int \frac{d^3k}{(2\pi)^3} \frac{m}{\mathbf{k}^2} \left(\frac{e^2}{4m^2} \right)^2 = -2 \frac{\alpha^2}{m^2} \frac{\Lambda}{m}. \quad (26)$$

This leads to a new contribution to $C^{(1)}$ and, consequently, to a correction to bound state energy equal to (see Eq.[24])

$$- |\Psi(0)|^2 \times -2 \frac{\alpha^2}{m^2} \frac{\Lambda}{m} = \frac{m\alpha^5}{4\pi} \frac{\Lambda}{m}. \quad (27)$$

Combining this with Eq.[25] yields a finite correction to the hyperfine splitting equal to $m\alpha^6/8$.

Before wrapping up this section, we would like to mention that there is yet another new ingredient appearing at order $m\alpha^6$. It has to do with the fact that, as we saw earlier, the Coulomb interaction does not increase the order (in powers of α) of the bound state diagrams. Although, in first order perturbation theory this is taken care of by the Schrödinger wavefunctions, in second order one must also sum up the Coulomb interactions in the *intermediate* state. In practice, this is done by using a closed form expression for the full Coulomb propagator which has been derived in both coordinate and momentum space [8].

6 Discussion

We have seen that there are two classes of contributions to bound state properties, one being characterized by the typical bound state momentum $p \approx m\alpha$ and one characterized by relativistic momenta $p \approx m$. Such a situation is ideal for the use of an effective field theory (in the decoupling scenario). NRQED is such a theory, with heavy scale Λ equal to the electron mass m . The use of NRQED greatly simplifies bound state calculations since it involves only nonrelativistic interactions in the bound state diagrams and incorporates the relativistic physics via the matching of conventional *scattering* amplitudes. The relative simplicity of the nonrelativistic interactions makes the bound state diagrams easy to evaluate whereas the QED interactions appear only in scattering amplitudes, which can be evaluated using conventional methods. This is to be contrasted with traditional approaches, the Bethe-Salpeter equation for example, which involve the fully relativistic theory in the bound state diagrams, leading to the difficulties discussed in Section 2.

We are finally able to understand in what way the order $m\alpha^4$ and $m\alpha^5$ corrections have a special status: the $m\alpha^4$ corrections come exclusively from *nonrelativistic* momenta (*i.e.* from NRQED diagrams) whereas the $m\alpha^5$ corrections come practically exclusively from *relativistic* momenta (*i.e.* from QED scattering diagrams). We say “practically” because, as we saw in the example derived above, there is a linear infrared divergence in the QED diagrams, showing that they are in fact sensitive to very low momenta. In fact this divergence is a pure threshold singularity, which is due to the fact that the diagrams are evaluated with external three-momenta set to zero. However, being a low-energy phenomenon, one expects this divergence to be reproduced by NRQED and we saw that this is exactly what happens, in the form of the Coulomb exchange diagram. But aside from this singularity, which gets canceled when matching QED and NRQED, the $m\alpha^5$ contribution originates entirely from QED scattering diagrams^{10 11}.

¹⁰Although we have explicitly shown this only for the annihilation diagram, this also holds for the $\mathbf{p} \cdot \mathbf{A}$ interaction; therefore *all* $\mathcal{O}(m\alpha^5)$ contributions to the hfs are purely relativistic.

¹¹It is in that sense that we call these contributions “purely” relativistic. Maybe a more appropriate terminology would be “bound state independent”. Notice that what we call “relativistic contributions” are sometimes referred to as “radiative corrections” in the

Let us now compare to the technique of Ref.[1]. For the $\mathcal{O}(m\alpha^4)$ correction, they consider the QED one-photon exchange in the scattering and annihilation channels, expanded them to lowest order in \mathbf{p}/m , and obtained the expressions Eq.[11] and Eq.[13]. At this order, this is exactly equivalent to using NRQED. In the language of NRQED, these interactions are found in the effective Lagrangian Eq.[3], which is obtained by taking the nonrelativistic limit of the QED Lagrangian. It is in that sense that we call the $\mathcal{O}(m\alpha^4)$ “purely” nonrelativistic; they are found directly from the effective Lagrangian.

Now consider the $\mathcal{O}(m\alpha^5)$ corrections. Once again, we restrict ourselves to the one-photon annihilation corrections for the sake of simplicity. In ref.[1], these corrections are obtained by sandwiching QED one-loop diagrams between wavefunctions, and taking the limit $\mathbf{p} \rightarrow 0$ in the QED spinors (threshold limit). In that limit, their calculation reduces to multiplying the one-loop threshold QED diagrams by the square of the wavefunctions evaluated at the origin. This is *almost* exactly what we find using NRQED. Indeed the $(m\alpha^5)$ term comes uniquely from the renormalization of the NRQED “bare” parameters, as we demonstrated explicitly in this paper. However, there is an important distinction between the two calculations. In [1], the photon mass dependence was discarded, with no further justification. But in NRQED, the λ dependence gets canceled, order by order in the matching procedure. Also, it is now easy to understand why the $\mathcal{O}(m\alpha^5)$ result for the ground state can be trivially generalized to ($l = 0$) states of arbitrary principal quantum number. Indeed, since the only effect of the bound state is to provide an overall normalization equal to the square of the wavefunction at the origin, the $\mathcal{O}(m\alpha^5)$ will carry the same dependence on n as $|\Psi(0)|^2$, namely it is proportional to $1/n^3$.

We are now in position to understand how the two approaches would differ at $\mathcal{O}(m\alpha^6)$, not only in the handling of the infrared divergences but also in the prediction of the finite term. We saw in Eq.[24] that, in contradistinction to the $\mathcal{O}(m\alpha^4)$ and $\mathcal{O}(m\alpha^5)$ corrections, the $m\alpha^6$ term contains finite contributions from both relativistic and nonrelativistic momenta. Notice that this is not simply a consequence of the presence of loops since the $\mathcal{O}(m\alpha^5)$ term already included integration over internal momenta. It has for origin a subtle interplay between relativistic and nonrelativistic flow of momenta

literature.

through the Feynman diagrams, interplay which is brought in evidence by the use of NRQED and its counting rules. Using the rules of [1] would yield the relativistic finite contribution only (in addition to infrared divergent terms which would have to be discarded without further justification).

The fact that nonrelativistic momenta play an important role at this order also has for consequence that it is no longer possible to consider Feynman diagrams containing only a fixed number of loops, as done in [1]. Indeed, as already mentioned in Section 5.3, at this order one must consider bound state diagrams with an infinite number of Coulomb interactions in the intermediate states. For example, were we to complete our calculation of the $\mathcal{O}(m\alpha^6)$ contribution due to the annihilation interaction in second order of perturbation theory, we would have to sum up the same diagram with any number of Coulomb vertices between the two contact interactions. This complication is directly at the origin of the issue of reducible *vs* irreducible Feynman diagrams in the Bethe-Salpeter approach. In NRQED, with the help of the Coulomb gauge, this problem is reduced to its most simple form since it is confined to the Coulomb interaction and the infinite sum can be performed using the expressions of [8].

Addendum

While writing this paper we became aware of [9], in which one contribution of $\mathcal{O}(m\alpha^6)$ is calculated. This contribution corresponds to the one-loop vacuum polarization correction to the exchange of two photons.

These diagrams, however, lead to purely relativistic corrections or, in other words, they contribute only to the coefficient A in Eq.[23]. This is because vacuum polarization is a highly virtual effect (notice that there is no vacuum polarization *per se* in NRQED; it only enters through the renormalization of the low energy theory's coefficients). This can be seen directly from the fact that the corresponding correction to the bound state energy is proportional to the square of the wavefunction at the origin (see Eqs[14-15] in [9]; notice that K is independent of the bound state momenta p and q). In that respect, the corrections due to these diagrams are similar to the $\mathcal{O}(m\alpha^5)$ terms; they are insensitive to bound state physics and can be treated using the formalism of [1] (especially since they are infrared finite). An example of a diagram contributing to $\mathcal{O}(m\alpha^6)$ that would be sensitive to low momenta would be, for example, the three photon exchange diagrams.

Acknowledgments

It is a pleasure to thank G. Peter Lepage for teaching me NRQED and Simon Dubé for many useful discussions concerning effective field theories. This work has been supported by the Natural Sciences and Engineering Research Council of Canada.

References

- [1] T. Zhang, L. Xiao and R. Koniuk, *Can. J. Phys.* **70**, 670 (1992).
- [2] NRQED was introduced in:
W. E. Caswell and G. P. Lepage, *Phys. Lett.* **167B**, 437 (1986).
For pedagogical introductions, see:
“What is renormalization?”, G.P. Lepage, invited lectures given at the TASI-89 Summer School, Boulder, Colorado; “Quantum Electrodynamics for Nonrelativistic Systems and High Precision Determinations of α ”, G.P. Lepage and T. Kinoshita, in *Quantum Electrodynamics*, T.Kinoshita ed. (World Scientific, Singapore, 1990); “NRQED in bound states: applying renormalization to an effective field theory”, P. Labelle, XIV MRST Proceedings (1992).
- [3] E.E. Salpeter and H.A. Bethe, *Phys. Rev.* **84**, 1232 (1951); see also review by S.J. Brodsky, in *Atomic Physics and Astrophysics*, edited by M. Chretien and E. Lipworth (Gordon and Breach, New York, 1969), Vol. I.
- [4] See for example: G.P.Lepage and B.A.Thacker, *Nucl.Phys.B* (Proc. Suppl.) **4** (1988), 199; B.A. Thacker and G.P.Lepage, *Phys. Rev.* **D 43** (1991), 196; C.T.H. Davies and B.A.Thacker, Ohio State University preprint DOE-ER-01545-554, May 1991.; G.P.Lepage *et al*, CLNS preprint 92/1136.
- [5] T. Appelquist and J. Carazzone, *Phys. Rev. D* **11**, 2856 (1975).
- [6] To see the one-photon annihilation $m\alpha^4$ and $m\alpha^5$ contributions to the hfs in positronium, consult

Itzykson and Zuber, *Quantum Field Theory*, McGraw-Hill, 1980, section 10.3.

- [7] C.P. Burgess and David London, McGill preprint 92/05, hep-ph preprint 9203216.
- [8] E.H. Wichmann and C.H. Woo, *J. Math. Phys.* **2**, 178 (1961); L. Hostler, *J. Math. Phys.* **5**, 591 (1961); J. Schwinger, *J. Math. Phys.* **5**, 1601 (1964).
- [9] Tao Zhang and Lixin Xiao, *Phys. Rev.* **A49**, 2411 (1994).

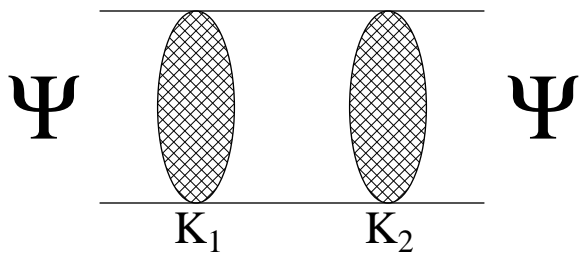


Figure 1(a)

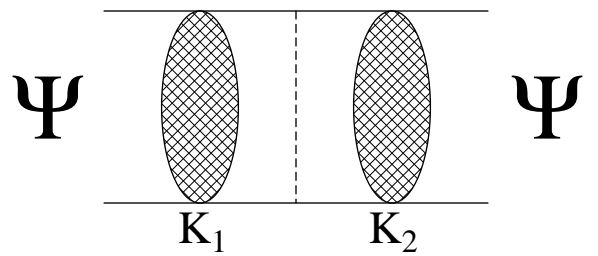


Figure 1(b)

This figure "fig1-1.png" is available in "png" format from:

<http://arxiv.org/ps/hep-ph/9407233v1>

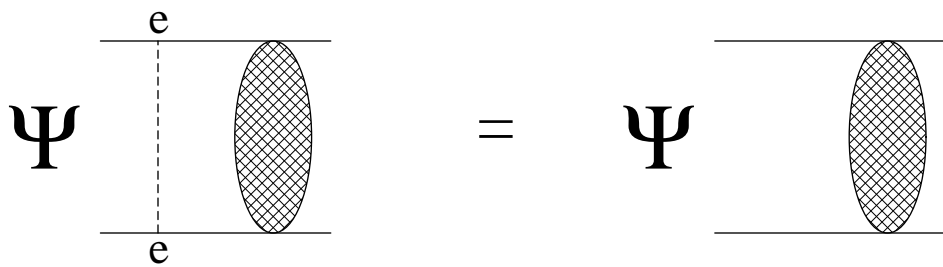


Figure 2

This figure "fig1-2.png" is available in "png" format from:

<http://arxiv.org/ps/hep-ph/9407233v1>

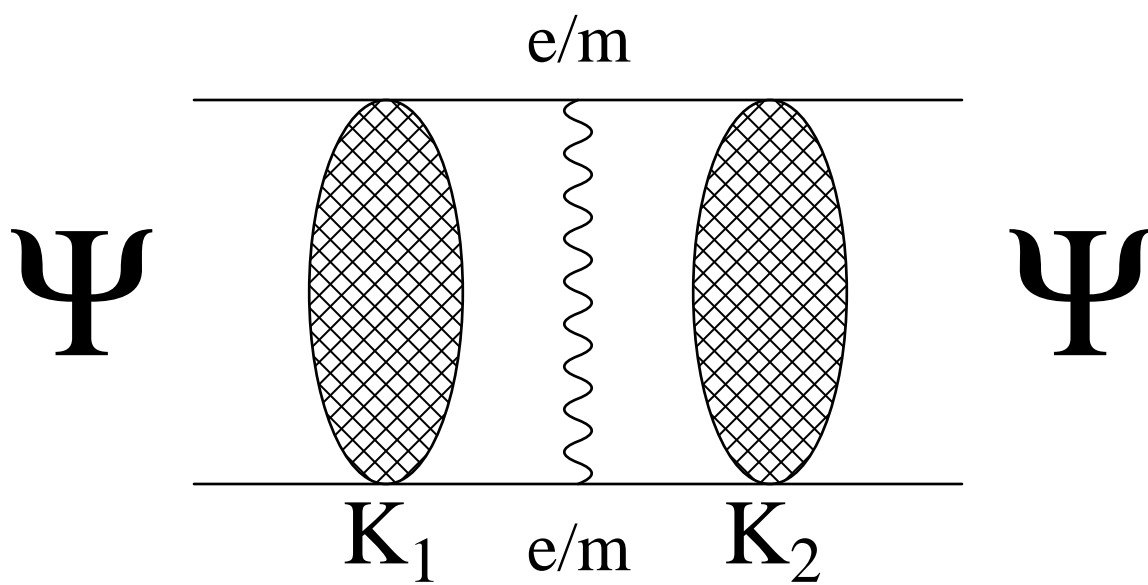
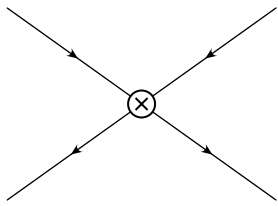


Figure 3

This figure "fig1-3.png" is available in "png" format from:

<http://arxiv.org/ps/hep-ph/9407233v1>



$(1 + C_1) + 1\text{-loop NRQED} =$

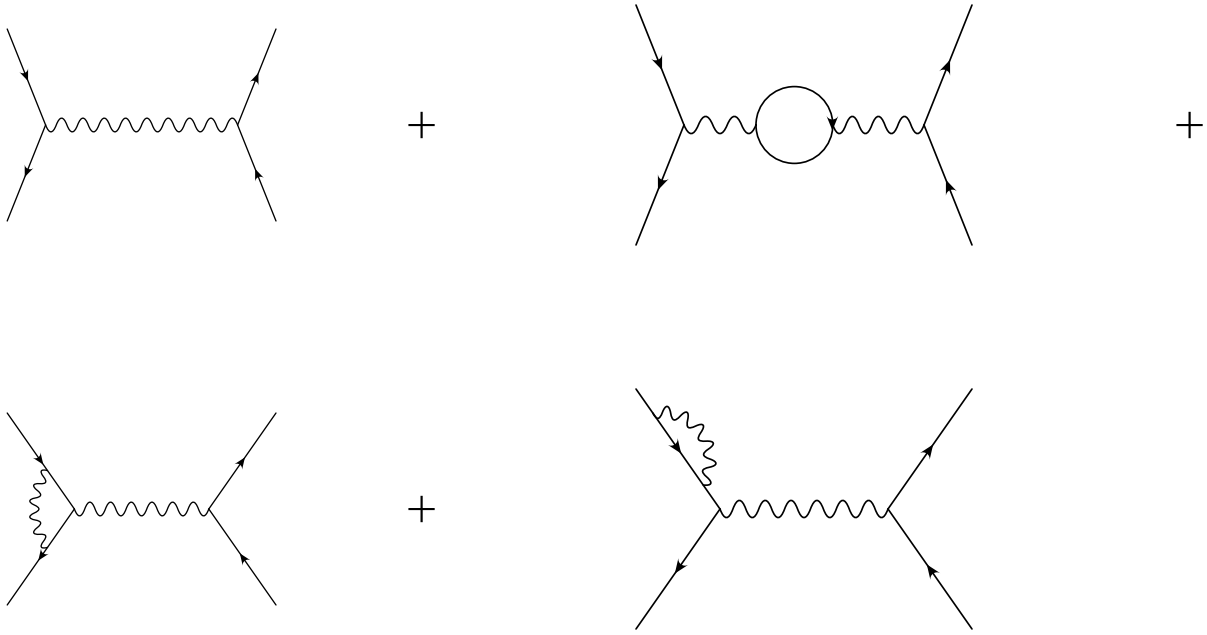


Figure 4

This figure "fig1-4.png" is available in "png" format from:

<http://arxiv.org/ps/hep-ph/9407233v1>

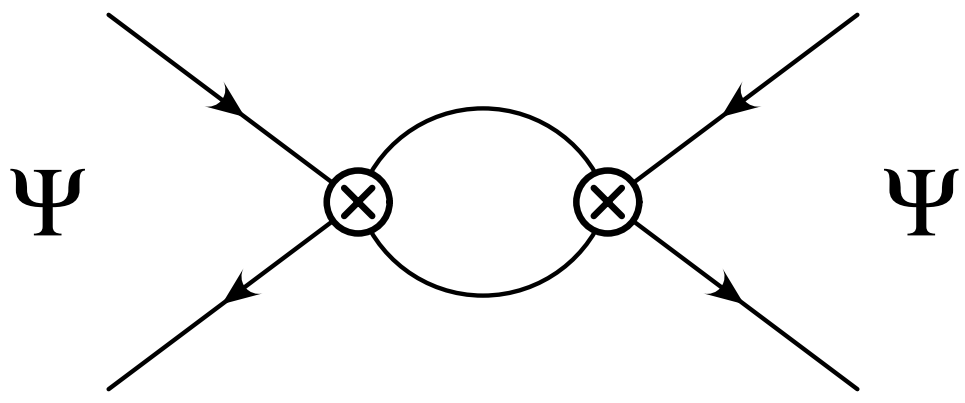


Figure 5

This figure "fig1-5.png" is available in "png" format from:

<http://arxiv.org/ps/hep-ph/9407233v1>